Clinical Brain MR Imaging Prescriptions in Talairach Space: Technologist- and Computer-Driven Methods

Kenneth L. Weiss, Hai Pan, Judd Storrs, William Strub,
Jane L. Weiss, Li Jia, and O. Petter Eldevik

BACKGROUND AND PURPOSE: **Variability in patient head positioning may yield substantial interstudy image variance in the clinical setting. We describe and test three-step technologist and computer-automated algorithms designed to image the brain in a standard reference system and reduce variance.**

METHODS: **Triple oblique axial images obtained parallel to the Talairach anterior commissure (AC)–posterior commissure (PC) plane were reviewed in a prospective analysis of 126 consecutive patients. Requisite roll, yaw, and pitch correction, as three authors determined independently and subsequently by consensus, were compared with the technologists' actual graphical prescriptions and those generated by a novel computer automated three-step (CATS) program. Automated pitch determinations generated with Statistical Parametric Mapping '99 (SPM'99) were also compared.**

RESULTS: **Requisite pitch correction (15.2° ± 10.2°) far exceeded that for roll (−0.6° ± 3.7°) and yaw (−0.9° ± 4.7°) in terms of magnitude and variance ($P < .001$). Technologist and computer-generated prescriptions substantially reduced interpatient image variance with regard to roll (3.4° and 3.9° vs 13.5°), yaw (0.6° and 2.5° vs 22.3°), and pitch (28.6°, 18.5° with CATS, and 59.3° with SPM'99 vs 104°). CATS performed worse than the technologists in yaw prescription, and it was equivalent in roll and pitch prescriptions. Talairach prescriptions better approximated standard CT canthomeatal angulations (9° vs 24°) and provided more efficient brain coverage than that of routine axial imaging.**

CONCLUSION: **Brain MR prescriptions corrected for direct roll, yaw, and Talairach AC-PC pitch can be readily achieved by trained technologists or automated computer algorithms. This ability will substantially reduce interpatient variance, allow better approximation of standard CT angulation, and yield more efficient brain coverage than that of routine clinical axial imaging.**

Although the Talairach anterior commissure (AC)–posterior commissure (PC) reference standard has been widely embraced by the neuroscience community, routine clinical brain MR imaging is still typically performed in the standard three orthogonal planes of the magnet with little regard to patient positioning. This approach makes interpretation and intrapatient or interpatient comparisons more difficult. Advances in MR imaging hardware and software have made patient-optimized oblique imaging in a standard reference frame more feasible and more readily implemented than when it was originally reported (1, 2).

Talairach and co-workers defined their intercommissural basal brain line as passing through the superior edge of the AC and the inferior edge of the PC (3) (Fig 1). The stereotactic atlas of Talairach and Tournoux, based on the brain of a 60-year-old right-handed French woman, has become the de facto standard reference almost universally used in functional brain imaging (1, 4). Researchers often transform their structural and functional data into Talairach space, which serves as a common coordinate reference system (2, 5).

The AC is composed of fiber bundles involved in interhemispheric transfer of temporal and orbitofrontal cortex axons. In the midline, the AC is immediately in front of the anterior columns of the fornix and inferoposterior to the rostrum of the corpus callosum

Received October 10, 2002; accepted after revision December 12.

From the Departments of Radiology, Psychiatry, and Biomedical Engineering (K.L.W., W.S.) and the Center for Imaging Research (K.L.W., H.P., J.S., J.L.W., L.J.), University of Cincinnati Medical Center, Cincinnati, OH; and the Department of Radiology, Neuroradiology Section, University of Michigan Medical Center, Ann Arbor (O.P.E.).

Address reprint requests to K.L. Weiss, MD, University of Cincinnati Medical Center, Department of Radiology, Cincinnati, OH 45267-0762.

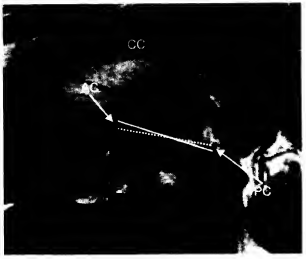

Fig 1. Midline sagittal FSE T2-weighted MR image (TR/TE, 3816/105$_{eff}$, echo train length, 16; section thickness, 4 mm; matrix, 512 × 256; FOV, 20 cm). The *solid line* and *dotted line* correspond to the Talairach and Schaltenbrand AC-PC reference lines, respectively. *AC* indicates the anterior commissure; *CC*, corpus callosum; and *PC*, posterior commissure.

(CC) (6). The PC consists of a variety of cell groups located anterior to the pineal region (7). It is posterior to central gray matter and rostral to the superior colliculi at the junction of the third ventricle and aqueduct of Sylvius (6). Pupillary light reaction and vertical eye movement is believed to be mediated by the PC (8).

As a slight modification of the Talairach reference, Schaltenbrand (9) and others have chosen the line connecting the middle of the AC and PC (Fig 1). An axial section passing through the Schaltenbrand reference line should depict both commissures simultaneously, whereas with the Talairach reference, the commissures are separately visualized on adjacent thin sections. Although perhaps more compelling from an MR imaging perspective, the Schaltenbrand line has not gained dominance over the more established Talairach reference.

The CC has also been proposed as a reference system, as it may be appreciated, even with low-resolution MR imaging, angiography, and positron emission tomography (10, 11). However, partly because of its relatively inconstant relationship to central gray matter nuclei, the CC has not achieved the status of the AC-PC line as a universal basal reference.

Itti et al (12) proposed automated image prescriptions based on surface mapping to a standard template brain. Their method, however, requires the acquisition of a nonclinical brain series and relies on surface features that may be variable and that may have an even more inconstant relationship to central gray matter nuclei than the CC. Moreover, their algorithm lacks a technologist-driven correlate that might permit more widespread adoption of their proposed reference standard.

To perform direct Talairach-referenced MR imaging examinations, Weiss et al (2) recently introduced a rapid three-step protocol. This consecutively corrected roll (y-rotation, ie, rotation about an axis along the anteroposterior direction), yaw (z-rotation, ie, rotation about an axis along the superoinferior direction), and pitch (x-rotation, ie, rotation about an axis along the left-right direction). To improve conspicuity of the AC and PC and to provide diagnostic coverage of the brain in the sagittal projection, we substituted a 15-section fast spin-echo (FSE) T2-weighted sequence for their single-shot FSE (SSFSE) imaging protocol and established this as our routine clinical protocol in October 2001.

Our prospective study was designed to test the efficacy of our revised protocol in the clinical setting and assess the potential for computer automation. We hypothesized that the protocol leads to a reduction in intersubject image variance, that it better approximates of the canthomeatal CT reference line, and that it provides more efficient brain coverage than standard axial imaging. Additionally, we hypothesized that each step of the protocol could be successfully automated.

Methods

Patient Selection

Institutional review board approval was obtained. We prospectively examined 126 consecutive patients (64 male, 62 female) who underwent imaging at our institution with the three-step clinical AC-PC protocol in a 2-week period from May 7, 2002, to May 21, 2002. The mean age of our subject population was 49.2 years ± 17.8 with a range of 17–89 years.

Imaging Protocol

All MR imaging studies were performed with one of two 1.5-T whole-body units (GE Medical Systems, Milwaukee, WI) at our institution. Patients were secured in the standard head coil after alignment was optimized by means of visual inspection. In the clinical protocol tested, a three-step technique sequentially corrected for patient roll, yaw, and pitch. First, a 2-second fast gradient-recalled echo (FGRE) coronal scout image was obtained, from which a similar 2-second axial oblique FGRE image was prescribed, with a correction for patient roll (Fig 2A). Subsequently, 15 double oblique sagittal T2 FSE sections were prescribed from this axial oblique image, with corrections for roll and yaw (Fig 2B). Finally, axial triple oblique images were prescribed from the adjusted midline sagittal image parallel to the AC-PC line, as described by Talairach (Fig 2C). Identical 4-mm, interleaved sections are typically obtained for all axial oblique sequences, simplifying setup and allowing for advanced prescription. Coronal sequencing perpendicular to the AC-PC line could also be prescribed in advance from the sagittal double oblique sequence or subsequently from the triple oblique axial series (2).

Criterion Standard Determination

To establish a criterion standard, independent blinded measurements of required roll, yaw and pitch correction were made by three coauthors (J.L.W., W.S., K.L.W., the last a board-certified radiologist with a Certificate of Added Qualification in neuroradiology) by using custom designed software. Corrections in a clockwise direction were assigned positive values, and counterclockwise corrections were assigned negative values.

For roll and yaw determination, the three coauthor measurements were averaged and 15% of cases (19 of 126 cases) with greatest coauthor variance were reexamined. These cases

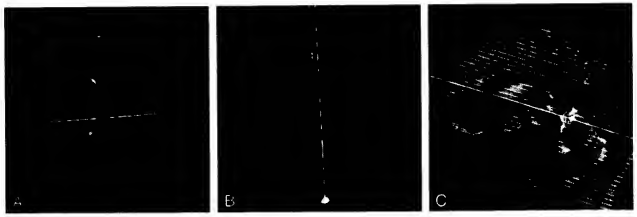

FIG 2. Sequential images from a single patient's three-step clinical AC-PC protocol.

A, Coronal FGRE localizer image (6/1.6; flip angle, 20°; section thickness, 7 mm; matrix, 256 × 192; FOV, 24 cm) for roll prescription. The *line* indicates the plane of the image in *B*.

B, Roll-corrected axial oblique FGRE localizer image (8/1.6; flip angle, 20°; section thickness, 7 mm; matrix, 256 × 192; FOV, 24 cm) for yaw prescription. The *thickest line* indicates the plane of the image in *C*.

C, Roll- and yaw-corrected double oblique T2-weighted FSE image ($3816/105_{eff}$; echo train length, 16; section thickness, 4 mm; skip, 1 mm; matrix, 512 × 256; FOV, 20 cm; NEX, 2; time, 1 minute 56 seconds) for pitch prescription. The *thickest line* indicates the Talairach reference plane used for subsequent triple oblique axial scans.

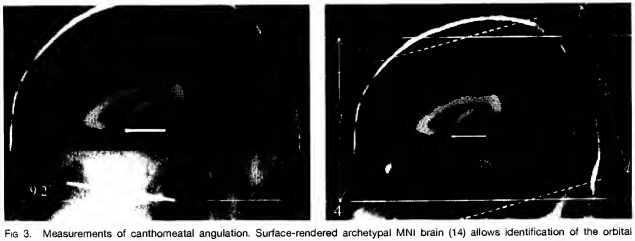

FIG 3. Measurements of canthomeatal angulation. Surface-rendered archetypal MNI brain (14) allows identification of the orbital canthus and the external acoustic meatus.

FIG 4. Requisite brain volume coverage: Talairach versus average axial sectioning for the archetypical MNI brain (14). *Solid lines* are Talairach referenced. *Dotted lines* correspond to an average patient head position oriented 15.1° counterclockwise from AC-PC. Measurements are in millimeters. Note the reduction in brain volume coverage afforded by Talairach obliquity compared with standard axial imaging.

were independently reexamined by each coauthor, and a 20% trimmed mean was computed to reduce the influence of outliers by discarding both the largest and the smallest measurement and by averaging the four remaining values for each discordant case.

For pitch, the custom software recorded *x*- and *y*-coordinate selections from the midsagittal image for the superior edge and center of the AC and for the inferior edge and center of the PC. For each image the greatest distance of any single observation from the mean was used as a score. Each of the three coauthors independently reexamined the 15% of cases (19 of 126) with highest score, and they also subsequently reviewed these cases as a group to achieve a consensus and to remove outliers (13).

Canthomeatal Pitch and Requisite Axial Coverage Determinations

To assess canthomeatal pitch relative to the Talairach AC-PC line, we retrospectively reviewed surface-rendered three-dimensional (3D) datasets from both the archetypical single individual Montreal Neurologic Institute (MNI) brain (14) and the averaged MNI brain (15), the latter obtained from 305 healthy volunteers. The angle subtended by a line drawn through the orbital canthus and external acoustic meatus and a line drawn through the superior edge AC and inferior edge PC were measured (Fig 3).

To assess requisite axial brain coverage, the distance from the foramen magnum (tonsillar tip) to the brain convexity was measured twice, once perpendicular to the Talairach AC-PC line and once perpendicular to a line representing the mean patient obliquity in our study. Measurements were made on the archetypical MNI brain (Fig 4), the average MNI brain, and an archetypically positioned patient from our study (14, 15).

Technologist Measurements

A total of 15 technologists imaged patients with the AC-PC protocol during the 2-week study period. Technologists of

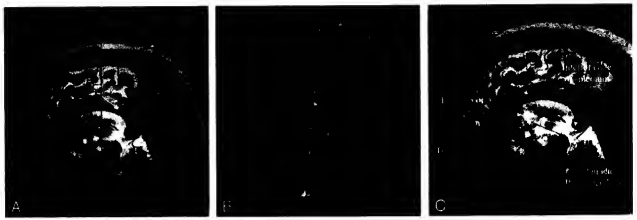

Fig 5. Illustration of CATS functionality.
A, APE to determine the positions of the scalp and CC by examining intensities along the central column of pixels from a midline sagittal T2-weighted image.
B, Automated contours and a bisecting line on a 2-second axial oblique T1-weighted gradient-recalled echo image. Note that brightest point lies within the cross section of the superior sagittal sinus (SSS) as a result of entry-flow phenomenon.
C, Outline of the CC, triangle search mask, and Talairach AC-PC reference line on a midline sagittal T2-weighted image.

record had a wide range of MR imaging expertise (ranging from students in training to chief technologists), and experience with the tested protocol varied from 1 day to 8 months. Technologist prescriptions were derived from the orientation information contained within the Digital Imaging and Communications in Medicine (DICOM) headers of the triple oblique clinical scans. These calculations were automated by using DCMTK (Kuratorium OFFIS; Oldenburg, Germany) and Matlab 6.1 (The MathWorks, Inc, Natick, MA).

Computer Algorithms

Computer algorithms were designed to emulate and potentially substitute for each step of the technologist driven three-step clinical protocol (2). These computer automated three-step (CATS) algorithms were implemented in Matlab 6.1 as C-language MEX extensions, and they were developed by using a training dataset of 48 randomly selected clinical brain MR imaging studies from our institution.

The roll and yaw algorithms used coronal or axial oblique 2-second FGRE images, respectively, to identify the sagittal sinus in cross section and to find lines through the sagittal sinus that bisect the brain. An automatic parameter estimation (APE) method found intensity thresholds for the scalp and skull by examining intensity peaks along the central column of pixels (Fig 5A). Boundaries for scalp, skull and brain regions of the image were then determined by using the contours based on these intensities, and the scalp and skull were stripped. Next, the algorithm identified the brightest point of the stripped image in a superior portion of the coronal image or in a posterior portion of the axial image. This point was presumably within the sagittal sinus. Roll or yaw was determined by optimizing the slope of a line passing through this point to approximately bisect the area of the brain (Fig 5B).

The pitch algorithm automatically determined the positions of the AC and PC from a single midline sagittal T2-weighted image and computed both Talairach and Schaltenbrand AC-PC reference lines. For pitch, CC was located by means of APE (Fig 5A), and its shape was used to predict the locations of the AC and PC. Two imaging features were extracted to locate the CC, AC, and PC: A contour was used to identify the boundary of the CC (Fig 5C), and a map of concavity points identified local minima. After the scalp and skull were removed, contour lines were used to determine the boundary of the CC. Then, the shape of the CC was used to locate the rostrum of corpus callosum (RCC) and the inferior edge of the splenium (IES), as well as to predict the location of the mammillary bodies (MB) by using the concavity map. The algorithm used a coarse to fine strategy to search for the AC and PC. The area roughly defined by the triangle formed by the RCC, IES, and MB was assumed to contain the AC and PC. Candidate positions for both were statistically estimated from the shape of the CC, and the two nearest concavity points were chosen as the AC and PC (Fig 5C). If no suitable concavity point was found, the estimate was used. Therefore, as long as the CC was identified, Talairach and Schaltenbrand AC-PC reference lines could be derived.

An alternate computer-based method to determine pitch is to minimize the difference between the 15-section double oblique sagittal T2-weighted FSE image obtained and a template T2-weighted dataset of known orientation. SPM'99 (Statistical Parametric Mapping '99; Wellcome Department of Cognitive Neurology, Institute of Neurology, London, England) is a freely available Matlab software package that implements this functionality for MR imaging. The T2-weighted template provided with SPM'99 and used in this study was derived from the MNI average brain (14–16). To facilitate direct comparisons to the pitch algorithm described previously, we assumed that technologists had adequately corrected for roll and yaw and trivially modified SPM'99 to allow affine normalization with rotation only for pitch. Parenthetically, because of the limited brain coverage afforded by the 15 sagittal sections, SPM'99 functioned erratically without this rotational constraint.

Statistical Analysis

Statistical analyses were performed in NCSS 2001 (NCSS and PASS; Number Cruncher Statistical Systems, Kaysville, UT; available at *www.ncss.com*) and Excel (Microsoft, Redmond, WA). For each angle prescription, deviation from the criterion standard measures precision and absolute deviation from the criterion standard was used to measure accuracy. To test whether accuracy in roll determination was influenced by patient yaw, we performed a Pearson correlation coefficient analysis.

Results

Criterion Standard Data Analysis

Interauthor variance (coauthor interobserver error) was low overall, with only a few measurements

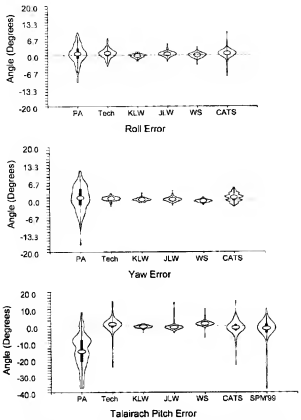

FIG 6. Violin plots of prescription errors. Technologist (*Tech*) and computer (*CATS* and *SPM'99*) methods are compared with physical alignment (*PA*). Spread narrowing indicates reduced image variability. (*KLW*, *JLW*, and *WS* are authors' initials.)

requiring review and consensus determination (Fig 6). Despite efforts to physically align the patients, most individuals demonstrated some degree of head roll and yaw. Mean roll was −0.6° ± 3.7°, and mean yaw was −0.9° ± 4.7° (Table 1).

In two pitch determinations, a consensus could not be reached, and a criterion standard was not established, leaving 124 cases for comparison with technologist and computer algorithm prescriptions. Talairach pitch was 15.2° ± 10.2°, and Schaltenbrand pitch was 9.4° ± 10.4°. Talairach pitch differed from Schaltenbrand pitch by 5.81°± 1.07°. Talairach and Schaltenbrand pitch values had similar precision, with similar SDs (10.2° and 10.4°, respectively) and similar ranges (48.3° and 48.3°, respectively) (Table 1). Pitch variance (104.2° Talairach and 107.5° Schaltenbrand) far exceeded that for roll (13.5°) or for yaw (22.4°) ($P < .001$) (Fig 6).

Canthomeatal Pitch and Requisite Axial Coverage

Retrospective review of surface-rendered 3D datasets from the archetypical MNI brain (14) and averaged MNI brain (305 healthy volunteers) (15) revealed that the canthomeatal pitch was approximately 9° steeper than the Talairach AC-PC line (Fig 3). Given our mean pitch correction of 15.1° ± 10.2°, axial oblique Talairach prescriptions better approximated standard CT canthomeatal angulation than routine axial imaging (9° vs 24°) and Schaltenbrand angulation (9° vs 15°).

The Talairach prescription also typically provides more efficient brain coverage than that of straight axial imaging. As illustrated in Figure 4, the required coverage for the archetypical MNI brain (14) is approximately 8.1 mm less by using Talairach (134.2 mm) compared with straight axial prescription (142.3 mm). Similarly, analysis of the averaged MNI brain (15) and our archetypical clinical case in which the patient pitch was 15.1° relative to the Talairach line demonstrated a savings of approximately 8.0 and 5.3 mm, respectively.

Technologist Results

Technologist prescriptions for roll, yaw, and pitch are summarized in Tables 1 and 2 and in Figure 6. As the clinical protocol required Talairach prescriptions, the technologists did not record Schaltenbrand observations. Thirteen technologists prescribed three or more studies (9.31 ± 6.05). The Pearson correlation coefficient between roll-determination accuracy and the patient's absolute yaw was 0.48.

Computer Results

Prescriptions for roll, yaw, and pitch are summarized in Tables 1 and 2 and in Figure 6. The Pearson correlation coefficient between the CATS roll-determination accuracy and the patient's absolute yaw was 0.13.

In five cases, CATS could not identify the CC, and thus, it was unable to determine pitch. Because one of these cases also lacked a criterion standard, 120 of the original 126 cases were available for full comparison to the 124 cases with a criterion standard. Schaltenbrand measurements were not obtained with SPM'99, because the brain template used was Talairach and not Schaltenbrand referenced.

All images were processed on a 2.0-GHz Pentium 4 PC (Dell, TX) running Windows 2000 Professional (Microsoft). Computer processing time for roll and yaw determination was less than 1 second per study. Pitch determination with our algorithm averaged 6.7 seconds ± 1.3 per study and approximately 20 seconds per study with the modified SPM'99 routine. A substantial portion of this performance difference resulted from the time needed to load the full 15-section dataset into memory for the SPM'99 method.

Comparison of Technologist and Computer Algorithms

Because of the presence of outliers, the paired *t* test may have been unreliable for our data. Instead, we chose to use the nonparametric sign or quantile test that is not heavily influenced by outliers or variations from a normal distribution (17). As can be seen in Figure 6, technologist- and CATS-generated prescriptions substantially reduced interpatient image variance with regard to roll, yaw, and pitch.

TABLE 1: Prescribed angulation

Algorithm*	N	Mean	Median	Variance	SD	IQR	Minimum	Maximum	Range
Roll									
CS	126	−0.60	−0.59	13.47	3.67	3.95	−9.17	10.59	19.75
Tech	126	0.11	0.00	16.75	4.09	4.47	−13.46	12.35	25.81
CATS	126	−0.12	−0.15	11.49	3.39	5.11	−6.06	6.73	12.79
Yaw									
CS	126	−0.86	−0.94	22.38	4.73	6.20	−11.17	17.26	28.43
Tech	126	−0.26	−0.32	20.02	4.47	6.00	−9.48	18.51	28.00
CATS	126	0.01	−0.61	18.80	4.34	6.78	−8.49	16.21	24.70
Talairach pitch									
CS	124	15.16	15.11	104.23	10.21	12.97	−8.13	40.20	48.34
Tech	126	15.59	15.25	99.59	9.98	14.28	−18.78	38.85	57.64
CATS	121	13.86	14.04	111.03	10.54	14.66	−10.39	41.42	51.81
SPM'99	126	11.95	10.96	60.56	7.78	10.80	−4.40	36.04	40.45
Schaltenbrand pitch									
CS	124	9.35	8.63	107.62	10.37	13.60	−14.62	33.69	48.31
CATS	121	9.97	9.02	115.37	10.74	14.36	−13.82	38.97	52.78

* CS indicates criterion standard; Tech, technologist; IQR, interquartile range.

TABLE 2: Deviation from the criterion standard

Algorithm*	N	Mean	Median	Variance	SD	IQR	Minimum	Maximum	Range
Roll									
PA	126	0.60	0.59	13.47	3.67	3.95	−10.59	9.17	19.75
Tech	126	0.71	0.78	3.42	1.85	1.99	−4.29	6.81	11.1
CATS	126	0.48	0.66	3.92	1.98	1.63	−8.21	9.37	17.6
Yaw									
PA	126	0.86	0.94	22.38	4.73	6.20	−17.26	11.17	28.43
Tech	126	0.59	0.63	0.65	0.81	0.97	−2.50	2.57	5.1
CATS	126	0.86	0.96	2.52	1.59	2.11	−2.40	4.73	7.1
Talairach pitch									
PA	124	−15.16	−15.11	104.23	10.21	12.97	−40.20	8.13	48.34
Tech	124	0.56	1.15	28.62	5.35	2.88	−24.62	20.68	45.3
CATS	120	−1.23	−1.11	18.52	4.30	3.60	−23.41	14.81	38.2
SPM'99	124	−3.14	−1.56	59.30	7.70	5.23	−37.96	9.88	47.8
Schaltenbrand pitch									
PA	124	−9.35	−8.63	107.62	10.37	13.60	−33.69	14.62	48.31
CATS	120	0.70	1.13	18.30	4.28	4.07	−20.41	15.48	35.9

* PA indicates physical alignment; Tech, technologist; IQR, interquartile range.

Discussion

The three-step Talairach prescription technique provides several potential advantages. The direct correction of roll and yaw facilitates interhemispheric comparison in the axial and coronal planes, respectively. Standardization of pitch further facilitates intersubject comparison. The Talairach reference is an obvious choice, as it has already become the de facto standard for neurostereotaxis and functional imaging studies. Locating critical structures may be simplified. The Rolandic fissure, for example, consistently passes between the vertical (coronal) AC and PC planes. It originates caudally 0.5 cm in front or behind the vertical AC and terminates in the midline approximately 1-cm posterior to the vertical PC (1, 2, 18). Direct visual correlation with standard brain atlases or integration with existing software referenced to Talairach space may be facilitated without the need for reformatting. Such postprocessing may be time consuming and unless isotropic 3D datasets are acquired, result in diminished in-plane resolution.

The Talairach reference line better approximates the canthomeatal line, which is routinely used for CT angulation, than either the Schaltenbrand line or the standard axial orientation. This improvement may facilitate the comparison of brain CT and MR images. Parenthetically, variation in patient's CT pitch prescriptions at our institution and at other centers is considerable. As such, it may be of benefit to study and standardize bony landmarks on lateral scout CT images that best approximate the canthomeatal or Talairach line. With CT, however, the radiation dose to the cornea and beam-hardening artifacts should also be considered.

Selecting the Talairach reference line allows for more efficient and consistent brain coverage than that typically obtained with conventional axial sectioning. The reduction of approximately 6 mm in requisite coverage translates to a savings of one or two images with our routine 4.0-mm sectioning. With the AC-PC protocol, most patients' brains are adequately imaged with 32 contiguous axial sections, resulting in a slight

overall reduction in acquisition time on our MR imaging system.

Potential disadvantages do exist. On average, switching to the Talairach reference adds approximately 15° ± 10° of angulation to the axial plane of the magnet. This may add stress to the gradient system, and the triple oblique orientation may not be currently compatible with all pulse sequences. Additionally, the paranasal sinuses and nasopharynx may not be as fully imaged with the axial oblique sequences. Furthermore, protocol requires technologist training or automated software integration and additional, albeit short, setup and imaging time. Given the average requisite pitch correction, comparison to previously obtained straight (nonreferenced) brain MR imaging studies may be more difficult.

Without additional training, most MR imaging technologists can reliably and rapidly correct for roll and yaw, with remarkable accuracy with the latter. If desired, better accuracy for the former might be achieved if the technologists were to use an iterative approach to role determination when subsequent yaw correction exceeds a certain threshold. For example, if absolute raw correction exceeds 5° (as in 34 of 126 patients), a 2-second double oblique coronal localizer could be prescribed from the axial oblique localizer image to serve as a better template for subsequent sagittal prescription. Given a correlation coefficient of only 0.48, however, use of this additional sequence may not be justified for technologists outside the research setting. Moreover, with an even smaller correlation coefficient of 0.13, this iterative approach does not appear to have appreciable value for the computer algorithm.

Although several technologists performed well, the average technologist versus the criterion standard pitch discordance was significantly higher than the intra-author observer error ($P < .001$). Technologist training beyond simply providing technique illustrations (2) might improve pitch-correction accuracy. Practice datasets derived from our 126 case studies may be helpful.

Both the technologist- and computer-driven methods notably reduced intersubject image variance in terms of roll, yaw, and pitch. However, because our study did not include infants or children, these results may not be generalized outside the adult population without further investigation. Nonetheless, as the CC, AC, and PC have attained a nearly adult configuration by 1 year of age, with minimal modification, we anticipate similar results beyond the first year and far better results than those achievable with single-template matching methods (19).

Although the CATS algorithm did not perform as well as the technologists in correcting yaw, the algorithm's mean absolute yaw error of only 1.46° ± 1.06° is believed to be within an acceptable range. CATS was more accurate than SPM'99 in correcting pitch, but it was unable to make a determination in four of 124 cases with criterion standard measurements. In such cases in which midline disease impaired delineation of the CC, the CATS algorithm could be extended to fall back to SPM'99-style template matching or to prompt for technologist prescription.

Although not studied, CATS is expected to provide better precision than that of the technologists when roll, yaw, and pitch correction are determined on follow-up patient studies. With minor modifications, the algorithm could also be used to automatically correct for interimage patient movement. Between imaging sequences, the 2-second FGRE coronal scout could be reacquired and compared with the original. If the computer detects interscan motion exceeding a certain threshold, the CATS algorithm could proceed with its 2-second FGRE axial oblique scout followed by a 2-second T2-weighted SSFSE midline double oblique localizer (2). Acquisition of an FGRE axial oblique scout image could be followed by a 2-second T2-weighted SSFSE midline double oblique localizer imaging (2). With a simple template-matching algorithm and the initially obtained midline sagittal T2-weighted FSE image constrained to translation and pitch rotation, interimage patient motion could be automatically compensated for. This scheme could potentially permit accurate interimage motion assessment in 3 seconds and automated triplanar correction, if required, in an additional 6 seconds.

Our study was a proof of principle. As successful, we are currently attempting to implement our CATS and motion-compensation algorithms on several different MR imaging platforms. Interfacing with proprietary MR imaging systems, however, poses technical challenges unique to each vendor.

Direct integration of automated prescription algorithms into clinical MR imaging systems may reduce setup times and allow precise, operator-independent implementation of a wide range of brain imaging protocols referenced to Talairach space. For example, on the basis of the orientation of the hippocampus in the average MNI brain, we can prescribe oblique imaging perpendicular to the hippocampus by simply angling 56° steeper than the Talairach AC-PC line (14).

Conclusion

Whether automated or technologist driven, we advocate the use of direct Talairach-referenced brain MR imaging prescriptions as a new clinical standard and encourage manufacturers to facilitate their implementation. Direct roll-, yaw-, and pitch-corrected standardized brain MR images can be achieved by trained technologists or by automated computer algorithms to considerably reduce interpatient image variance. The widely used Talairach AC-PC reference is recommended. Compared with straight axial imaging, this reference better approximates standard CT obliquity and provides more efficient brain coverage. Adoption of the Talairach AC-PC reference standard may lead to more reproducible and readily interpretable clinical brain MR images.

Acknowledgments

We gratefully acknowledge Paul R. Toney and his team of MR imaging technologists for their assistance in this study and for the excellent clinical imaging they provide.

References

1. Talairach J, Tournoux P. **Co-planar stereotaxic atlas of the human brain.** New York: Thieme; 1988:122
2. Weiss KL, Dong Q, Weadock WJ, et al. **Multiparametric color-encoded brain MR imaging in talairach space.** *RadioGraphics* 2002; 22:3e
3. Talairach J, Tournoux P. **Practical examples for the use of the atlas in neuroradiologic examinations. In**: Talairach J, Tournoux P, eds. *Co-Planar Stereotaxic Atlas of the Human Brain*. New York: Thieme; 1988:19–36
4. Raichle ME. **A brief history of human functional brain mapping.** In: Toga AW, Mazziota JC, Frackowick SJ, eds. *Brain Mapping the Systems*. San Diego: Academic Press: 2000;33–68
5. Mega MS. **Brain mapping in dementia. In**: Toga AW, Mazziotta JC, Frackowiak SJ, eds. *Brain Mapping The Disorders*. Academic Press: San Diego; 2000: 218–234
6. Carpenter MB. **Olfactory pathways Hippocampal formation and the amygdala. In**: Carpenter MB, ed. *Core Text of Neuroanatomy*. Baltimore: Williams and Wilkins; 1985:416
7. Blanchet B. **The anatomy and the MRI anatomy of the interhemispheric cerebral commissures.** *AJNR Am J Neuroradiol* 1995;22: 237–251
8. Bianchi R, Gioia M. **Accessory oculomotor nuclei of man, III: the nuclear complex of the posterior commissure—a Nissl and Golgi study.** *Acta Anatomica* 1993;146:53–61
9. Schaltenbrand G, Bailey P, eds. *Introduction to Stereotaxis with an Atlas of Human Brain*. Vol 1–2. Stuttgart: Thiene; 1959
10. Olivier A. **Intergration de l'angiographie numerique de la resonance magnetique de la tomodenistometrie et de la tomographie par emission de positrons en stereotaxie.** *Rev Electroencephlogr Neurophysiolo Clin* 1987;17:25–43
11. Sun Yu H, Paik CH. **Anatomic labeling of PET brain images with automatic detection of AC and PC.** *J Dig Imaging* 1998;11:56–58
12. Itti L, Chang L, Thomas E. **Automatic scan prescription for brain MRI.** *Magn Reson Med* 2001;45:486–494
13. Iglewicz B, Hoaglin D. **How to detect and handle outlier.** In: *The ASQC Basic References in Quality Control: Statistical Techniques*. Milwaukee: Quality Press
14. Collins DL, Zijdenbos AP, Kollokian V, et al. **Design and construction of a realistic digital brain phantom.** *IEEE Trans Med Imaging* 1998;17:463–468
15. Evans AC, Collins DL, Mills SR, et al. **3D statistical neuroanatomical models from 305 MRI volumes.** *Proc IEEE Nucl Sci Symp Med Imaging Conf* 1993:1813–1817
16. Friston KJ, Ashburner J, Frith CD, et al. **Spatial registration and normalization of images.** *Human Brain Mapping* 1995;2:165–189
17. Milton JS, Arnold JC. *Introduction to Probability and Statistics: Principles and Applications for Engineering and Computing Sciences*. 3rd ed. New York: McGraw-Hill; 1995:282–288
18. Roberts T, Rowley H. **Mapping of the sensorimotor cortex: functional MR and magnetic source imaging.** *AJNR Am J Neuroradiol* 1997;18:871–880
19. Dietrich RB. **Maturations, myelination, and dysmyelination**. In: Stark D, Bradley W Jr, eds. *Magnetic Resonance Imaging*. 3rd ed. St Louis: Mosby; 2000:1425–1447